Progress In Electromagnetics Research, PIER 99, 383–404, 2009

DARK SOLITON BEHAVIORS WITHIN THE NONLINEAR MICRO AND NANORING RESONATORS AND APPLICATIONS

S. Mitatha

Hybrid Computing Research Laboratory, Faculty of Engineering
King Mongkut's Institute of Technology Ladkrabang
Bangkok 10520, Thailand

Abstract—We propose some fascinating results regarding dark soliton pulse propagation within the nonlinear micro and nano waveguides. The system consists of nonlinear micro and nanoring resonators whereby the dark soliton is input into the system and travels within the waveguide. A continuous dark soliton pulse is sliced into smaller pulses by the nonlinear effect which is known as chaos. The nonlinear behaviors such as chaos, bistability and bifurcation are analyzed and discussed. The broad area of applications such as dark-bright soliton conversion and power amplification, binary code generation by the dark-bright soliton pair, dark soliton trapping and millimeter wave generation are proposed and discussed. The biggest advantage is that, where security is the most important consideration, power amplification can be used to perform the long distance link.

1. INTRODUCTION

Nonlinear behaviors of light pulse traveling within a fiber optic ring resonator have been analyzed [1], where the nonlinear Kerr type is the major effect within the fiber ring [2]. They have shown that such nonlinear behaviors can be beneficial for different forms such as bistability switching, signal security and digital encoding [3]. However, the power attenuation of the signal output becomes a problem in the long distance link. For security purposes, a dark soliton pulse is recommended to overcome such a problem so the problem of power attenuation can be solved. In addition, the low level signal detection of the dark soliton is another problematic aspect of behavior. Dark

Corresponding author: S. Mitatha (kmsomsak@kmitl.ac.th).

soliton is one of the soliton properties where the soliton amplitude vanishes during the propagation in transmission line. Therefore, dark soliton detection is extremely difficult. To date, several papers have investigated the dark soliton behaviors [4–8] and one shows an interesting result in that the dark soliton can be converted into a bright soliton and finally detected. This means that the dark soliton penalty can be used as a communication carrier so that it can be retrieved by the dark-bright soliton conversion [6]. Recently, a soliton pulse has been used to produce fast switching [7, 9] localized within a nano-waveguide [8] and it was reported that they have designed a system which consists of micro and nanoring resonators. In this paper, we present the interesting results, where a dark soliton pulse can be formed with nonlinear behaviors within the designed waveguide, which means that the usage of dark soliton is possible and if we can use such behaviors in an advantageous way then we can have reasonable detection power. The dark soliton valley signal is always low output level, which is difficult to detect, while the dark-bright conversion is required [9].

Dark and bright soliton behaviors have been widely investigated in different forms [10, 11]. The use of soliton, i.e., bright soliton in long distance communication links has been in operation for nearly two decades. However, some questions still need to be answered in the area of communication safety, whereas the use of a dark soliton pulse within a microring resonator for communication security has been studied [12]. In this research dark/bright soliton is used to enhance confidentiality in communication links. Dark soliton is one of the soliton properties, where the soliton amplitude vanishes or minimizes during the propagation in media, therefore, the detection of dark soliton is difficult. The investigation of dark soliton behaviors has been reported [13] and one has shown the interesting result that the dark soliton can be stabilized [14] and converted into bright soliton [15] and finally detected. This means that we can use the dark soliton to perform the communication transmission for security, whereas the required information can be retrieved by the dark-bright soliton conversion. In fact, we are looking for a simple technique that can be employed to detect the dark soliton. Yupapin and Suwancharoen have reported [16] the interesting results of light pulse propagation within a nonlinear microring device where the transfer function of the output at the resonant condition is derived and used. They found that the broad spectrum of light pulse can be transformed to the discrete pulses. In this paper, we have shown that after the dark soliton is input and sliced for the purpose of noisy signals for security purposes within the nonlinear ring resonator system this can be transmitted into the

transmission link safely. The required users can retrieve the original signal via an add/drop filter by choosing to retrieve either bright or dark soliton pulses. However, the device parameters are the given keys for the end users and these can be used to form the device that can be used to retrieve the signals in the link or network. The conversion signal amplification is also a better technique and with this we found that significant amplified signals can be achieved. The novelty is that the soliton behavior within a micro and nano ring resonator has been investigated, wheras all parameters are based on the practical device parameters [19, 20], which is shown the potential of applications.

2. OPERATING PRINCIPLES

An optical soliton is recognized as a powerful laser pulse, which can be used to enlarge the optical bandwidth when propagating within the nonlinear microring resonator. Moreover, the superposition of self-phase modulation (SPM) soliton pulses can maintain the large power output. Initially, the optimum energy is coupled into the waveguide by a larger effective core area device, i.e., a ring resonator then the smaller one is connected to form the stopping behavior. The filtering characteristic of the optical signal is presented within a ring resonator, where the suitable parameters can be controlled to obtain the required output energy. To maintain the soliton pulse propagating within the ring resonator, suitable coupling power into the device is required, whereas the interference signal has a minor effect compared to the loss associated with the direct signal passing through.

We are looking for a stationary soliton pulse, which is introduced into the microring or a multi-stage microring resonator system as shown in Fig. 1, the input optical field (E_{in}) of the dark soliton pulse

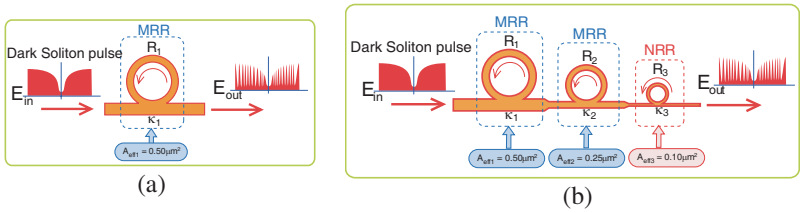

Figure 1. A schematic of an all optical dark soliton pulse system, R_s: Ring radii, κ_s: Coupling coefficients, MRR: Microring resonator, NRR: Nanoring resonator.

input is given by [17].

$$E_{in} = A \tanh\left[\frac{T}{T_0}\right] \exp\left[\left(\frac{z}{2L_D}\right) - i\omega_0 t\right] \tag{1}$$

where A and z are the optical field amplitude and propagation distance, respectively. T is the soliton pulse propagation time in a frame moving at the group velocity, $T = t - \beta_1 * z$, where β_1 and β_2 are the coefficients of the linear and second order terms of Taylor expansion of the propagation constant. $L_D = T_0^2/|\beta_2|$ is the dispersion length of the soliton pulse. T_o in the equation is the soliton pulse propagation time at the initial input. Where t is the soliton phase shift time, the frequency shift of the soliton is ω_0. This solution describes a pulse that keeps its temporal width in variance as it propagates, and thus is called a temporal soliton. When a soliton peak intensity $\left(\left|\beta_2/\Gamma T_0^2\right|\right)$ is given, then T_o is known. For the soliton pulse in the microring device, a balance should be achieved between the dispersion length (L_D) and the nonlinear length (L_{NL}= $(1/\mathrm{g}\Gamma\phi_{NL})$, where $\Gamma = n_2 * k_0$, is the length scale over which dispersive or nonlinear effects make the beam wider or narrower. For a soliton pulse there is a balance between dispersion and nonlinear lengths, hence $L_D = L_{NL}$.

When light propagates within the nonlinear material (medium), the refractive index (n) of light within the medium is given by:

$$n = n_0 + n_2 I = n_0 + \left(\frac{n_2}{A_{eff}}\right) P, \tag{2}$$

where n_0 and n_2 are the linear and nonlinear refractive indexes, respectively. I and P are the optical intensity and optical power, respectively. The effective mode core area of the device is given by A_{eff}. For the microring and nanoring resonators, the effective mode core areas range from 0.50 to 0.1 $\mu\mathrm{m}^2$ [6, 16].

When a soliton pulse is input and propagated within a microring resonator as shown in Fig. 1, which consists of a series of microring resonators. The resonant output is formed, thus, the normalized output of the light field is the ratio between the output and input fields ($E_{out}(t)$ and $E_{in}(t)$) in each roundtrip, which can be expressed as [18].

$$\left|\frac{E_{out}(t)}{E_{in}(t)}\right|^2 = (1-\gamma)\left[1 - \frac{\left(1-(1-\gamma)\,x^2\right)\kappa}{\begin{array}{c}(1-x\sqrt{1-\gamma}\sqrt{1-\kappa})^2 \\ +4\,x\sqrt{1-\gamma}\sqrt{1-\kappa}\sin^2(\frac{\phi}{2})\end{array}}\right] \tag{3}$$

The close form of the Equation (3) indicates that a ring resonator in this particular case is very similar to a Fabry-Perot cavity, which

has an input and output mirror with a field reflectivity, $(1-\kappa)$, and a fully reflecting mirror. κ is the coupling coefficient, and $x = \exp(-\alpha L/2)$ represents a roundtrip loss coefficient, $\phi_0 = kLn_0$ and $\phi_{NL} = kLn_2 |E_{in}|^2$ are the linear and nonlinear phase shifts, $k = 2\pi/\lambda$ is the wave propagation number in a vacuum where L and α are a waveguide length and linear absorption coefficient, respectively. In this work, the iterative method is introduced to obtain the results as shown in the Equation (3) and similarly, when the output field is connected and input into the other ring resonators.

After the signals are multiplexed with the generated chaotic noise, then the chaotic cancellation is required by the individual user. To retrieve the signals from the chaotic noise, we propose to use the add/drop device with the appropriate parameters. This is given in the details that follow. The optical circuits of ring-resonator add/drop filters for the throughput and drop port can be given by Equations (4) and (5), respectively [19].

$$\left|\frac{E_t}{E_{in}}\right|^2 = \frac{\begin{array}{c}(1-\kappa_1) - 2\sqrt{1-\kappa_1}\cdot\sqrt{1-\kappa_2}e^{-\frac{\alpha}{2}L}\cos(k_nL) \\ +(1-\kappa_2)\,e^{-\alpha L}\end{array}}{\begin{array}{c}1+(1-\kappa_1)(1-\kappa_2)\,e^{-\alpha L} \\ -2\sqrt{1-\kappa_1}\cdot\sqrt{1-\kappa_2}e^{-\frac{\alpha}{2}L}\cos(k_nL)\end{array}} \tag{4}$$

and

$$\left|\frac{E_d}{E_{in}}\right|^2 = \frac{\kappa_1\kappa_2 e^{-\frac{\alpha}{2}L}}{\begin{array}{c}1+(1-\kappa_1)(1-\kappa_2)\,e^{-\alpha L} \\ -2\sqrt{1-\kappa_1}\cdot\sqrt{1-\kappa_2}e^{-\frac{\alpha}{2}L}\cos(k_nL)\end{array}} \tag{5}$$

here E_t and E_d represent the optical fields of the throughput and drop ports respectively. $\beta = kn_{eff}$ is the propagation constant, n_{eff} is the effective refractive index of the waveguide and the circumference of the ring is $L = 2\pi R$, here R is the radius of the ring. In the following, new parameters will be used for simplification: $\phi = \beta L$ is the phase constant. The chaotic noise cancellation can be managed by using the specific parameters of the add/drop device so that the required signals can be retrieved by the specific users. κ_1 and κ_2 are coupling coefficient of add/drop filters, $k_n = 2\pi/\lambda$ is the wave propagation number for a vacuum and the waveguide (ring resonator) loss is $\alpha = 0.5\,\mathrm{dBmm}^{-1}$. The fractional coupler intensity loss is $\gamma = 0.1$. In the case of the add/drop device, the nonlinear refractive index is neglected.

3. SOLITON NONLINEAR BEHAVIORS

To begin the concept, we use only one ring resonator to form the nonlinear behaviors of a dark soliton. The schematic diagram of the

proposed system is as shown in Figs. 1(a) and 1(b). A dark soliton pulse with 50 ns pulse width, maximum power at 0.65 W is input into the system. The suitable ring parameters are used, for instance, ring radii $R_1 = 10.0\,\mu\text{m}$. In order to make the system compatible with the practical device [6, 16], the selected parameters of the system are fixed to $\lambda_0 = 1.55\,\mu\text{m}$, $n_0 = 3.34$ (InGaAsP/InP), $A_{eff} = 0.50$, $0.25\,\mu\text{m}^2$ and $0.10\,\mu\text{m}^2$ for a microring and nanoring resonator, respectively, $\alpha = 0.5\,\text{dBmm}^{-1}$, $\gamma = 0.1$. The coupling coefficient (kappa, κ) of the microring resonator is 0.009. The nonlinear refractive index is $n_2 = 2.2 \times 10^{-13}\,\text{m}^2/\text{W}$. In this case, the wave guided loss used is $0.5\,\text{dBmm}^{-1}$. The input dark soliton pulse is sliced into a smaller signal spreading over the spectrum as shown in Fig. 2 (middle). This shows that the large bandwidth signal is generated within the ring device. However, in this region the signal level is very low or vanishes completely at about 0.85–0.15×10^4 for each roundtrip and this is called a stop band.

The plot of nonlinear behaviors is shown in Fig. 2, where the plot between output and input power (intensity) is seen. When the input intensity is increased then bistability, bifurcation and chaos occur. For example, the first instance of bistability occurrs when

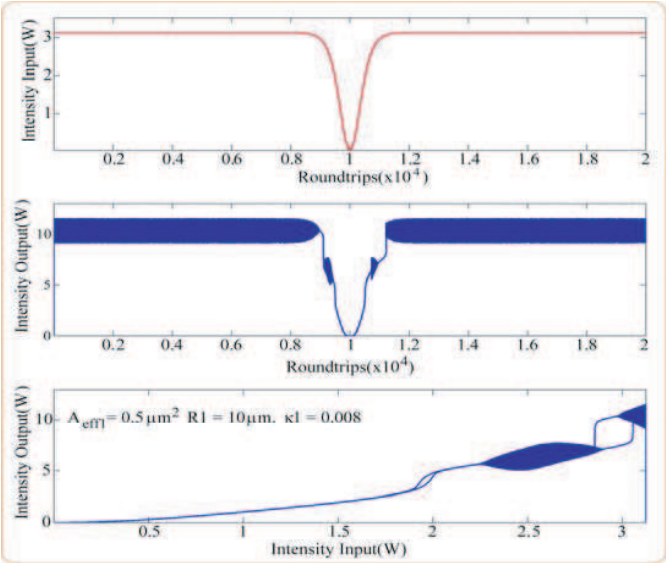

Figure 2. Simulation results obtained when a dark soliton pulse is input into a microring resonator, where $R_1 = 10\,\mu\text{m}$, $A_{eff1} = 0.50\,\mu\text{m}^2$, $\kappa_1 = 0.009$.

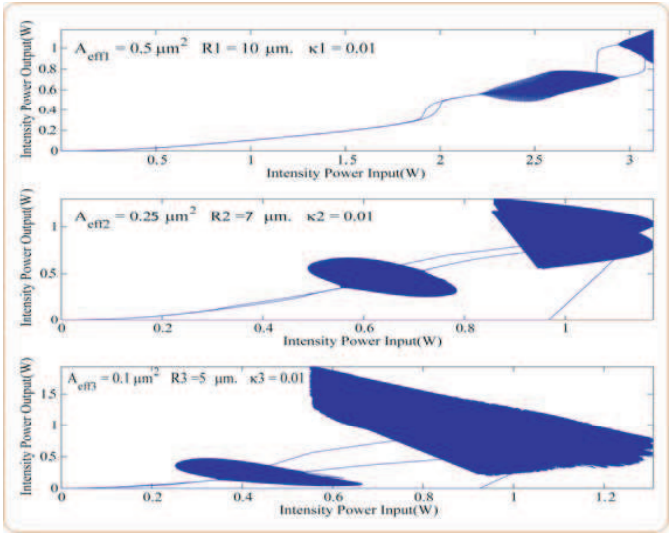

Figure 3. Simulation results of a dark soliton pulse propagating in a microring resonator system, where $R_1 = 10\,\mu\text{m}$, $A_{eff1} = 0.50\,\mu\text{m}^2$, $R_2 = 7\,\mu\text{m}$, $A_{eff2} = 0.25\,\mu\text{m}^2$, $R_3 = 5\,\mu\text{m}$, $A_{eff3} = 0.10\,\mu\text{m}^2$, $\kappa_1 = 0.01$ and $\kappa_2 = \kappa_3 = 0.01$.

the input intensity is between 1.8–2.0 W. Similar results are obtained, when a dark soliton pulse is input into a microring resonator, where the parameters used are $R_1 = 10\,\mu\text{m}$, $A_{eff1} = 0.50\,\mu\text{m}^2$, $\kappa_1 = 0.0030$ and $\kappa_1 = 0.050$ as shown in Fig. 3. The attempt in using a dark soliton pulse propagating into a micro and nanoring system is as shown in Fig. 1(b) and the result obtained is as shown in Fig. 3. The parameters used are (a) $R_1 = 10\,\mu\text{m}$, $R_2 = 5\,\mu\text{m}$, $R_3 = 2.5\,\mu\text{m}$, center wavelength at 1,550 nm, and (b) $R_1 = 10\,\mu\text{m}$, $R_2 = 7\,\mu\text{m}$, $R_3 = 5\,\mu\text{m}$, center wavelength at 1,550 nm. The coupling coefficients are the same, which is equal to 0.01. In Fig. 3, a dark soliton pulse is input into a microring resonator system, where the parameters used are $R_1 = 10\,\mu\text{m}$, $A_{eff1} = 0.50\,\mu\text{m}^2$, $R_2 = 7\,\mu\text{m}$, $A_{eff2} = 0.25\,\mu\text{m}^2$, $R_3 = 5\,\mu\text{m}$, $A_{eff3} = 0.10\,\mu\text{m}^2$ and $\kappa_1 = 0.01$ and $\kappa_2 = \kappa_3 = 0.01$. By using the control light concept, light can be trapped within the waveguide. For example, the control of input power after a soliton propagation within the system for a certain roundtrip is possible, where the input power can be adjusted to the values which can keep the trapped light localized within the ring resonator.

4. DARK-BRIGHT SOLITONS CONVERSION

In operation, a dark soliton pulse with 50 ns pulse width, the maximum power of 0.65 W is input into the dark-bright solitons conversion system as shown in Fig. 4. The suitable ring parameters are used, for instance,

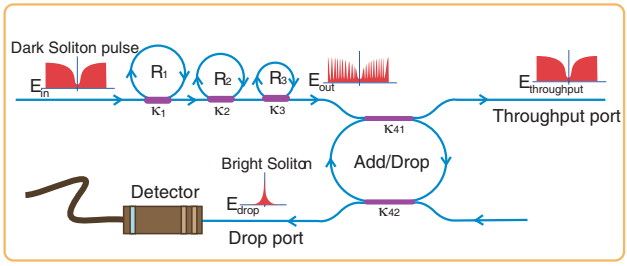

Figure 4. A schematic of a dark-bright soliton conversion system, where R_s: Ring radii, κ_s: Coupling coefficients, κ_{41} and κ_{42} are the add/drop coupling coefficients.

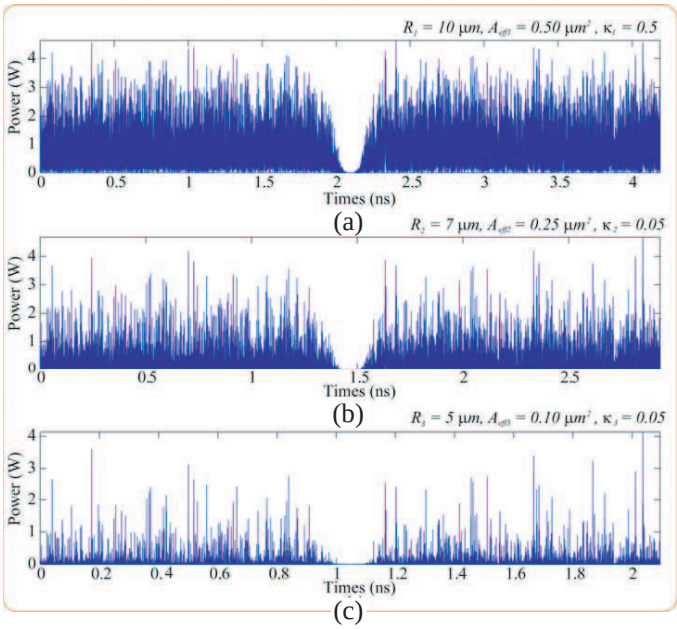

Figure 5. Simulation results of the soliton signals within the ring resonator system, where (a) in ring R_1, (b) in ring R_2 and (c) in ring R_3.

ring radii $R_1 = 10.0\,\mu m$, $R_2 = 7.0\,\mu m$, and $R_3 = 5.0\,\mu m$. In order to make the system compatible with the practical device, the selected parameters of the system are fixed to $\lambda_0 = 1.55\,\mu m$, $n_0 = 3.34$ (InGaAsP/InP). The light source used is the modulated Gaussian continuous wave. The effective core areas are $A_{eff} = 0.50,\ 0.25\,\mu m^2$ and $0.10\,\mu m^2$ for a microring and nanoring resonator [8], respectively. The waveguide and the coupling loses are $\alpha = 0.5\,dBmm^{-1}$, $\gamma = 0.1$, respectively, and the coupling coefficients (kappa, κ) of the microring resonator range from 0.05 to 0.90. However, more parameters are used as shown in the figures. The nonlinear refractive index is $n_2 = 2.2 \times 10^{-13}\,m^2/W$. In this case, the wave guided loss used is $0.5\,dBmm^{-1}$. The input dark soliton pulse is sliced into the smaller signals as shown in Fig. 5(a).

Figures 5(b) and 5(c) are the output signals of the filtering signals within the rings R_2 and R_3. We find that the output signals from R_3 are smaller than from R_1, which is more difficult to detect when it is used in the link. In fact, the multi-stage ring system is proposed due to the different core effective areas of the rings in the system, where the effective areas can be transferred from $0.50\,\mu m^2$ to $0.10\,\mu m^2$ with some

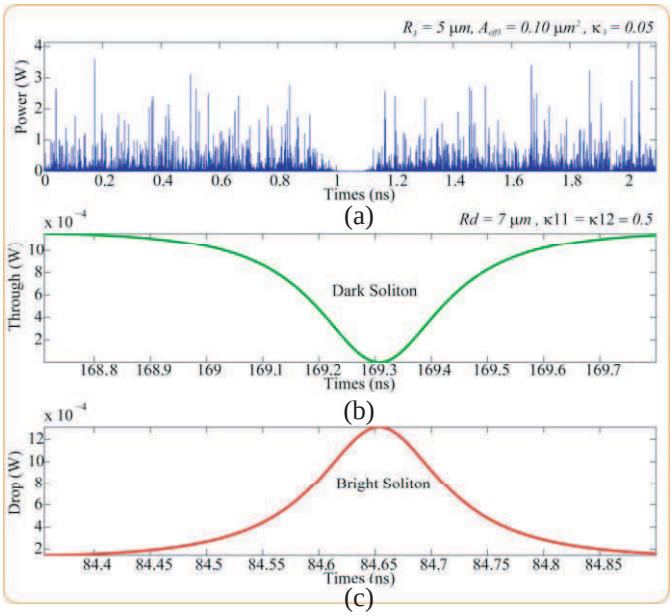

Figure 6. Simulation results of the optical solitons, where (a) the signals in R_3, (b) a dark soliton and (c) a bright soliton. The input dark soliton power is 0.65 W, $\kappa_1 = 0.5$, $R_d = 10\,\mu m$.

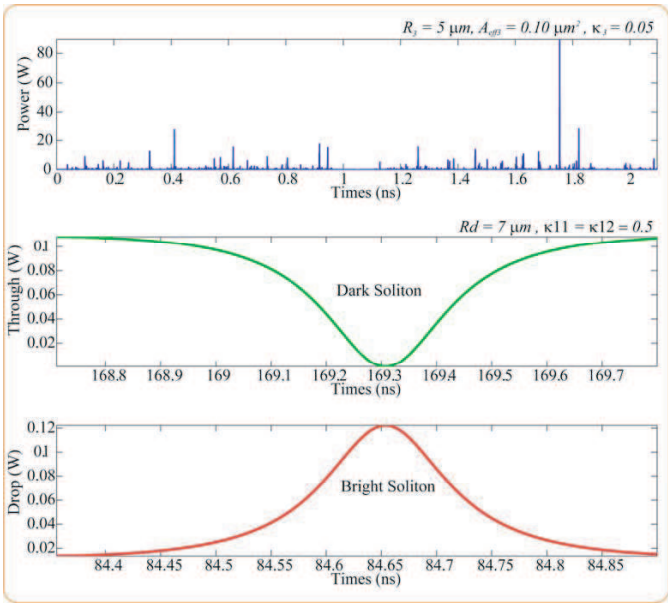

Figure 7. Simulation results of the optical solitons, where (a) the signals in R_3, (b) a dark soliton and (c) a bright soliton. The input dark soliton power is 0.65 W, $\kappa_1 = 0.9$, $R_d = 10\,\mu$m.

losses. The soliton signals in R_3 are entered in the add/drop filter so the dark-bright solitons conversion can be performed by using Eqs. (4) and (5). Results obtained when a dark soliton pulse is input into a micro and nanoring resonator system are as shown in Figs. 6 and 7. The parameters used are the same as in Fig. 5, where the only change is the add/drop filter parameters. The add/drop filter is formed by two couplers and a ring radius (R_d) of 10 μm, the coupling constants (κ_{11} and κ_{12}) are the same values (0.50). When the add/drop filter is connected to the third ring (R_3), the dark-bright soliton conversion is achieved and seen. The bright soliton and dark soliton are detected by the throughput and drop ports as shown in Fig. 4, respectively.

5. SOLITON AMPLIFICATION

The dark-bright soliton amplification system is as shown in Fig. 1(b). Firstly, when the bright soliton system is operated, the large bandwidth within the microring device can be generated by using a bright soliton pulse input into the nonlinear microring resonator as shown in Fig. 8. Similarly, the input dark soliton pulse is sliced into a smaller signal

spreading over the spectrum as shown in Fig. 9, which shows that the large bandwidth signal is generated within the first ring device. A soliton pulse with 50 ns pulse width, maximum power at 0.65 W is input into the system. Results obtained when a bright soliton pulse is input into the ring resonator system, when the parameters used are $R_1 = 10\,\mu\text{m}$, $A_{eff1} = 0.50\,\mu\text{m}^2$, $R_2 = 7\,\mu\text{m}$, $A_{eff2} = 0.25\,\mu\text{m}^2$, $R_3 = 5\,\mu\text{m}$, $A_{eff3} = 0.10\,\mu\text{m}^2$ and $\kappa_1 = 0.2$ and $\kappa_2 = \kappa_3 = 0.05$ result in a continuous spectra output 25 times larger than the input obtained and seen in Fig. 8(c), secondly, a dark soliton pulse is input into a microring resonator system within NRR, where the parameters used are $R_1 = 10\,\mu\text{m}$, $A_{eff1} = 0.50\,\mu\text{m}^2$, $R_2 = 7\,\mu\text{m}$, $A_{eff2} = 0.25\,\mu\text{m}^2$, $R_3 = 5\,\mu\text{m}$, $A_{eff3} = 0.10\,\mu\text{m}^2$ and $\kappa_1 = 0.2$ and $\kappa_2 = \kappa_3 = 0.05$, then a dark soliton pulse is sliced into the smaller signals as shown in Fig. 9(a). Figs. 9(b) and 9(c) are the output signals of the filtering signals within the rings R_2 and R_3. Results obtained when a dark soliton pulse is input into a micro and nanoring resonator system as shown in Fig. 1(b). The continuous spectra output with 25 times larger than the input is obtained, which is shown in Fig. 9(c). The coupling coefficients are given as shown in the figures. In operation, more amplification can

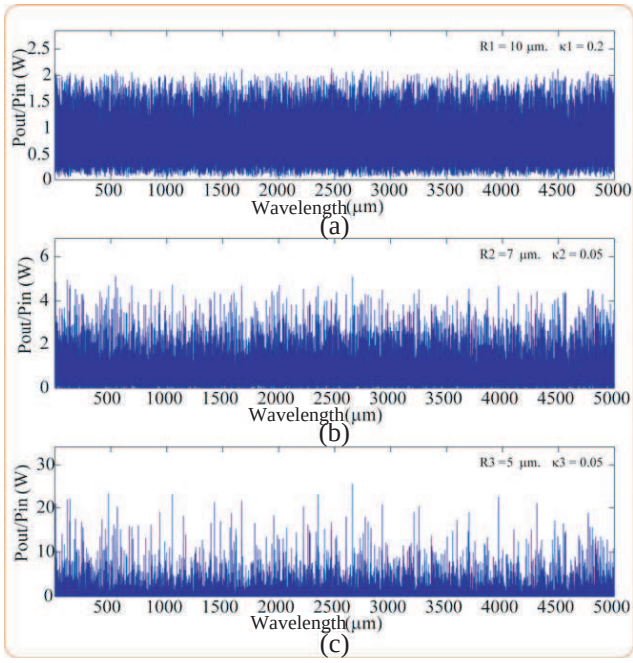

Figure 8. Simulation results of a bright soliton pulse is input into a microring resonator system for within NRR.

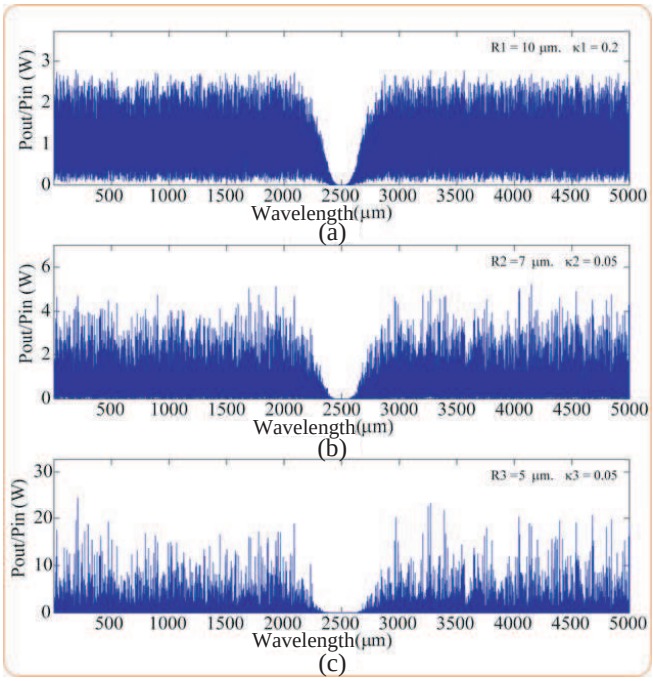

Figure 9. Simulation results of a dark soliton pulse is input into a microring resonator system for within NRR.

be obtained by using the nanoring resonator instead of the microring resonator. The results obtained for the amplification effect of dark soliton depends on the system consisting of the parameters in Fig. 9. In principle, the dark soliton amplification can also be employed.

6. RANDOM ENCODING VIA A DARK-BRIGHT SOLITON PAIR

In the operation as shown in Fig. 4, the proposed system can be used to generate the chaotic signal by using the first microring resonator and the cancellation of the chaotic signal can be achieved by using the add/drop filter (multiplexer) with the appropriate parameters. To obtain more power, which is suitable for a long distance link, the soliton pulse is recommended to be used for chaotic signal generation. In Figs. 6 and 7, the dark-bright conversion signals can be obtained by using the add/drop filters at drop ports 1, 2 and 3 of the add/drop filters R_4, R_5 and R_6. In principle, the conversion dark soliton, i.e.,

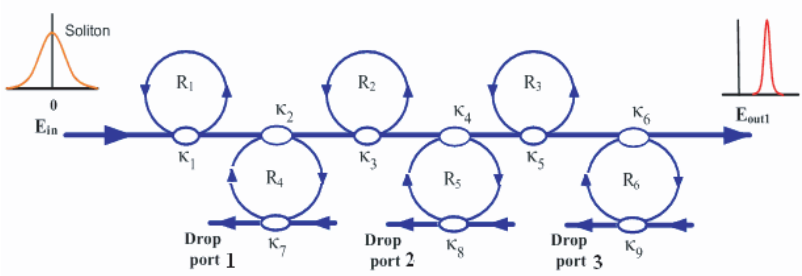

Figure 10. Schematic diagram of microring devices and add/drop multiplexers in the communication link.

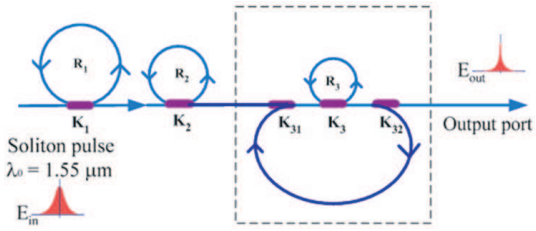

Figure 11. A schematic of an all optical dark soliton pulse system, R_s: Ring radii, κ_s: Coupling coefficients, κ_{31} and κ_{32} are coupling losses.

bright soliton is easier to detect than the dark one, where the retrieved information of the dark soliton can be obtained by the bright soliton. For the use in random code techniques, the detected dark soliton indicates the hidden one (bright soliton), which means that we can propose such a behavior for a random detection technique. As shown in Fig. 10, the random detection can be operated so that the detected signals at the drop ports imply that the signals in the transmission line are in the network. This concept can be proposed for the non-polarized entangled photon pair, which is more reliable than the polarization scheme for cryptography applications.

7. SOLITON TRAPPING

The schematic diagram of the proposed system is as shown in Fig. 11. Fig. 12 shows a result that was obtained by using a bright soliton. A bright soliton pulse with 20 ns pulse width, peak power at 500 mW is input into the system. The suitable ring parameters are used, for instance, ring radii $R_1 = 16.0\,\mu\text{m}$, $R_2 = 16.5\,\mu\text{m}$, and $R_3 = 4\,\mu\text{m}$.

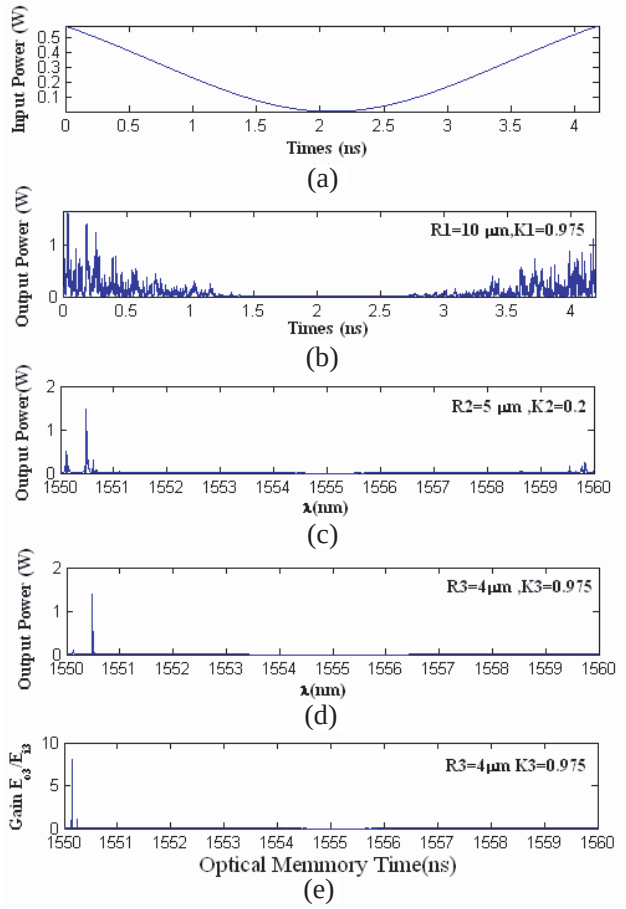

Figure 12. Simulation results obtained when a dark soliton pulse is input into a micro and nanoring resonator system, where the parameters used are (a) $R_1 = 10\,\mu\text{m}$, $R_2 = 5\,\mu\text{m}$, $R_3 = 2.5\,\mu\text{m}$, center wavelength at 1,550 nm, and (b) $R_1 = 10\,\mu\text{m}$, $R_2 = 5\,\mu\text{m}$, $R_3 = 4\,\mu\text{m}$, center wavelength at 1,550 nm and $\kappa_1 = \kappa_3 = 0.975$, $\kappa_2 = 0.2$, with 20,000 roundtrips.

The selected parameters of the system are fixed to $\lambda_0 = 1.55\,\mu\text{m}$, $n_0 = 3.34\,(\text{InGaAsP/InP})$, $A_{eff} = 0.50$, $0.25\,\mu\text{m}^2$ and $0.10\,\mu\text{m}^2$ for a microring and nanoring resonator, respectively, $\alpha = 0.5\,\text{dBmm}^{-1}$, $\gamma = 0.1$. The coupling coefficient (kappa, κ) of the microring resonator ranged from 0.20 to 0.975. The nonlinear refractive index is $n_2 = 2.2 \times 10^{-13}\,\text{m}^2/\text{W}$. In this case, the wave guided loss used is

$0.5\,\mathrm{dBmm}^{-1}$. The input soliton pulse is sliced into a smaller signal spreading over the spectrum as shown in Fig. 12(b) which shows that a large bandwidth signal is generated within the first ring device. We find that the large bandwidth signal does not occur when the Gaussian pulse is input into the same system. Figs. 12(c) and (d) show the decrease in spectral width of the output signals, where the parameters used are $R_2 = 16.5\,\mu\mathrm{m}$, $R_3 = 4\,\mu\mathrm{m}$.

Results obtained when a dark soliton pulse is input into a micro and nanoring resonator system as shown in Fig. 12. The parameters used are (a) $R_1 = 10\,\mu\mathrm{m}$, $R_2 = 5\,\mu\mathrm{m}$, $R_3 = 2.5\,\mu\mathrm{m}$, center wavelength at $1.55\,\mu\mathrm{m}$, and (b) $R_1 = 10\,\mu\mathrm{m}$, $R_2 = 5\,\mu\mathrm{m}$, $R_3 = 4\,\mu\mathrm{m}$, center wavelength at $1.55\,\mu\mathrm{m}$ and $\kappa_1 = \kappa_3 = 0.975$, $\kappa_2 = 0.2$, with 20,000 roundtrips. The other interesting property of the dark soliton pulse is that the localized behavior of the dark soliton pulse, which

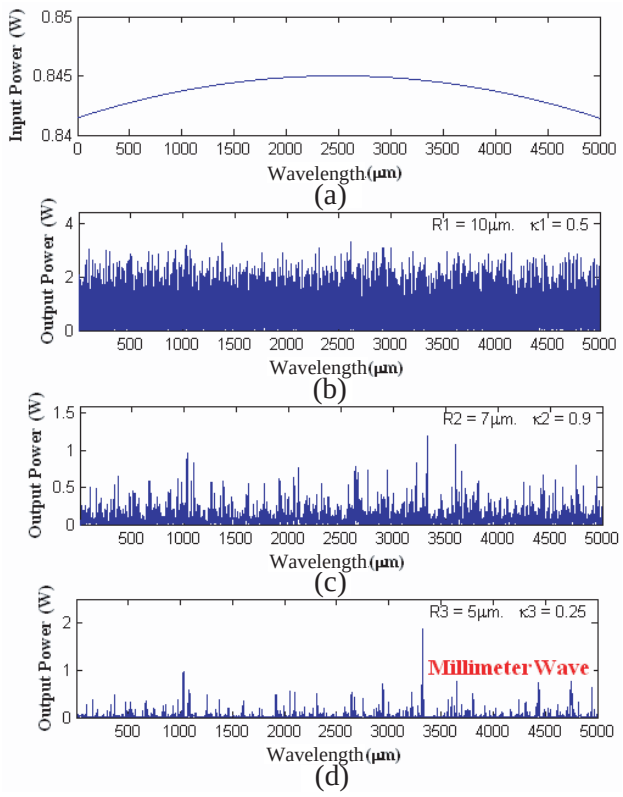

Figure 13. Simulation results obtained when a bright soliton pulse is input into a microring resonator, the millimeter wave is obtained.

occurred when the roundtrip time stopped or the stored light pulse switching time vanished (small group velocity). The stopping dark soliton concept is formed when the constant gain of the tuned light pulse is achieved as shown in Fig. 12(e). We have found that the tuned pulse gain recovery can be obtained by connecting the nanoring device into the system (i.e., R_2), therefore, the coupling loss is introduced due to the different core effective areas between micro and nanoring devices, which is located in the wavelength between 1.5502–1.5503 μm. However, we have already described that the other ring parameters are also very important to keep stopping light pulse behavior. We can conclude that the tuned dark soliton pulse can be stored or stopped in the nanoring device when the output gain reaches a constant value

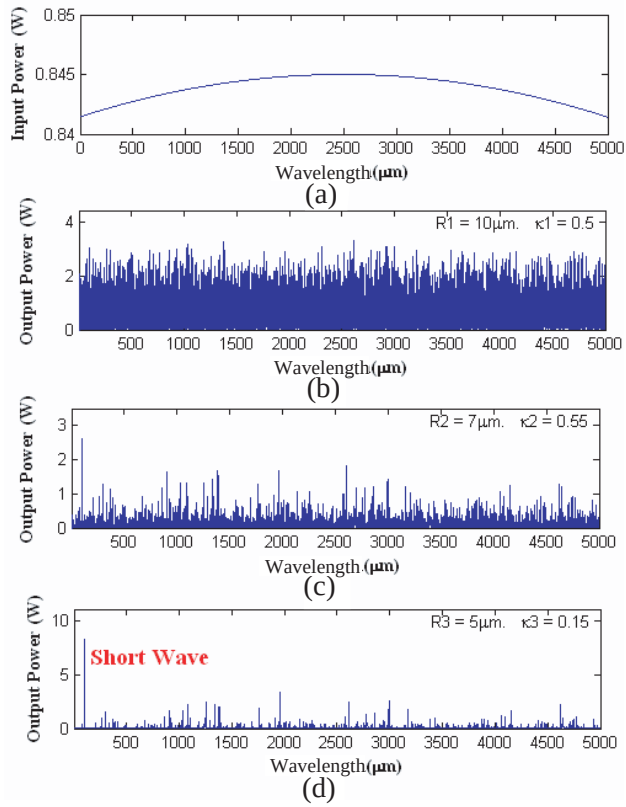

Figure 14. Simulation results obtained when a bright soliton pulse is input into a microring resonator, the short wave filtering signal is obtained.

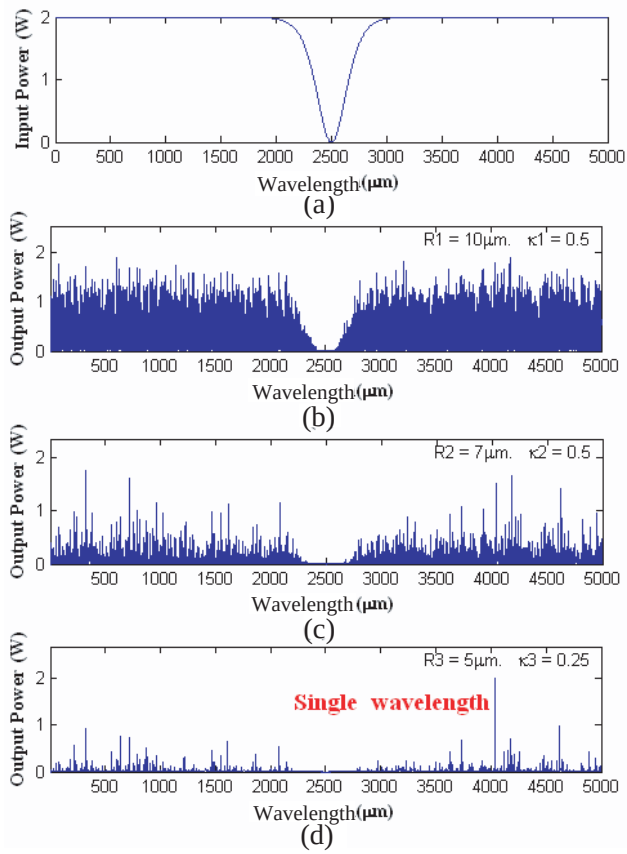

Figure 15. Simulation results obtained when a dark soliton pulse is input into a microring resonator, the dominant millimeter wave is obtained.

which is time independent, as shown in Fig. 12(e). In principle, when the soliton behavior known as self phase modulation **(SPM)** is performed then the balance between the dispersion and nonlinear length phase shift occurs which induces the dark soliton pulse gain recovery when the light pulse slows down and completely stops within a ring R_3.

8. SUB-MILLIMETER WAVES GENERATION

In principle, the large bandwidth signals within the microring device can be generated by using a soliton pulse input into the nonlinear

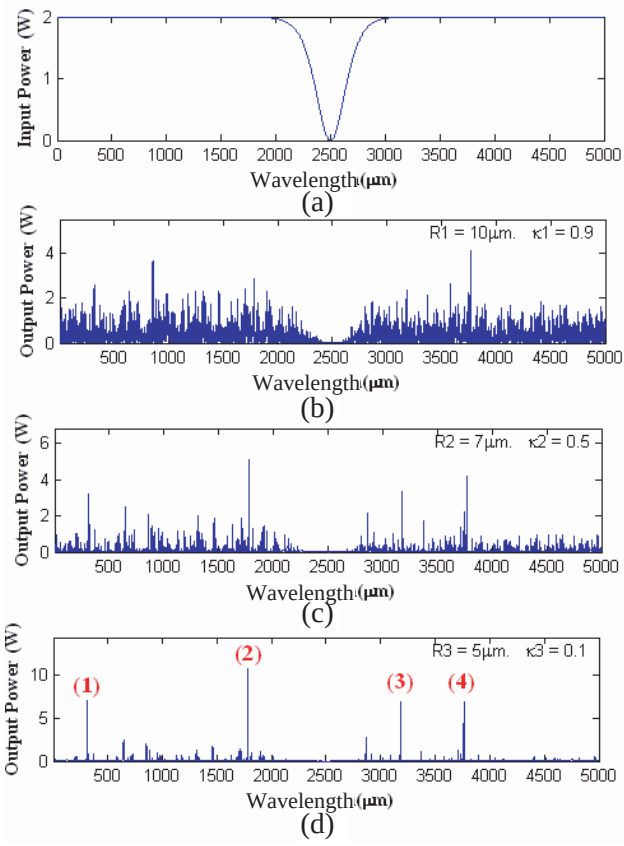

Figure 16. Simulation results obtained when a dark soliton pulse is input into a microring resonator, the short wave filtering signal is obtained (1).

microring resonator. The schematic diagram of the proposed system is as shown in Fig. 1(b). Firstly, a bright soliton pulse with 50 ns pulse width, peak power at 650 mW is input into the system. The suitable ring parameters are used, for instance, ring radii $R_1 = 10.0\,\mu\text{m}$, $R_2 = 7.0\,\mu\text{m}$, and $R_3 = 5.0\,\mu\text{m}$. The selected parameters of the system are fixed to $\lambda_0 = 1.55\,\mu\text{m}$, $n_0 = 3.34$ (InGaAsP/InP), $A_{eff} = 0.50$, $0.25\,\mu\text{m}^2$ and $0.10\,\mu\text{m}^2$ for a microring and nanoring resonator, respectively, $\alpha = 0.5\,\text{dBmm}^{-1}$, $\gamma = 0.1$. The coupling coefficient (kappa, κ) of the microring resonator ranged from 0.25 to 0.9. The nonlinear refractive index is $n_2 = 2.2 \times 10^{-13}\,\text{m}^2/\text{W}$. In this case, the wave guided loss used is $0.5\,\text{dBmm}^{-1}$. The input soliton pulse is

sliced into a smaller signal spreading over the spectrum as shown in Fig. 12(a), which shows that a large bandwidth signal is generated within the first ring device. We find that the large bandwidth signal does not occur when the Gaussian pulse is input into the same system. Secondly, a dark soliton pulse with 50 ns pulse width, maximum power at 2 W is input into the system. The suitable ring parameters are used, for instance, ring radii $R_1 = 10.0\,\mu m$, $R_2 = 7.0\,\mu m$, and $R_3 = 5.0\,\mu m$. The other parameters used are the same as in the bright soliton case. The coupling coefficients are given as shown in the figures.

In application, we propose two concepts, where firstly, the continuous spectrum can be generated by using the bright soliton as shown in Fig. 13. The generation of optical output within the nano-waveguide with the maximum power of 2 W is achieved. The wavelength sources are ranged from a few hundred nanometers to millimeters. This means the use of a ring resonator to generate the white light spectra and amplification is possible. The amplified power of continuous spectrum can be performed with a good white light source which is in large demand for many applications. Secondly, the output obtained from the bright and dark solitons are as shown in Figs. 13–16. They have shown the interesting results, where the generation of maximum output power of 10W is achieved.

The output wavelengths range from short wave, microwave, sub-millimeter and millimeter waves. Furthermore, the good separation band between short wave and millimeter wave is formed by the dark soliton result. This means that the bandwidth separation can be used to form a good guard band which is a requirement in transmission. However, in application, the required signals can be filtered and form the simultaneous generation of the short and millimeter waves within the remarkably simple system. In practice, short wave is required

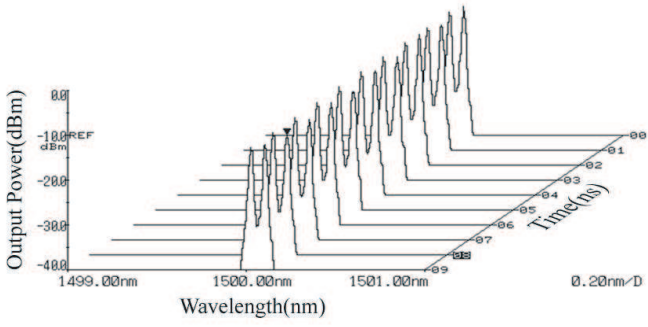

Figure 17. Experimental result shows a generated temporal dark soliton pulse.

in the communication concept via a radio link, where the object is signal security. The millimeter wave is useful when the radio signal is transmitted via the optical fiber link. Thus, our proposed systems have shown the promising results which can be fabricated and increase signal security and can be used in future applications.

9. DISCUSSION AND CONCLUSION

We also have the experimental result of dark soliton generation as shown in Fig. 17, where the temporal dark soliton is formed in the gap between a Brillouin pump (BP) signal at 1.5 μm and Stokes signal at 1.50009 μm, which have peak powers of −12 dBm. The generated beam is seen to be stable with no fluctuations over a test period of 10 minutes [20].

Fujii et al. [21] have shown that a typical propagation length at around sub-millimeter of optical fields can be confined into an approximately $100 \times 200\,\mathrm{nm}^2$ cross section waveguide. The other published works [17, 22] also confirm the same results. The behaviour of the guide mode when the quality factor is smaller than 1, it is well described by Yupapin et al. [18].

In conclusion, we have shown that the large bandwidth of an arbitrary wavelength of a soliton pulse can be enlarged and stored within a nano-waveguide which is then available for trapping within the waveguide. Also, the selected light pulse can be trapped and controlled by light. Furthermore, the large signal amplification, due to the effects of a dark soliton pulse in the nonlinear waveguide, may introduce unexpected applications, where the use for signal security in long distance communication and networks can be performed. The novelty of the presented work is that the small system of the integrated or embedded devices can be formed the proposed requirement, where the problem of signal amplification and security can be solved. Moreover, the idea of trapping a dark soliton may introduce the concept of storing a dark soliton which is a new concept for this particular subject.

ACKNOWLEDGMENT

We would like to give our appreciation to Prof. Dr. P. P. Yupapin and Dr. J. Arnold from King Mongkut's Institute of Technology for their help of manuscript proof reading.

REFERENCES

1. Ferreira, M. F. S., "Nonlinear effects in optical fibers: Limitations and benefits," *Proc. SPIE*, Vol. 6793, 02, 2007.
2. Akhmanov, S. A. and S. Y. Nikitin, *Physical Optics*, 657, Oxford University Press, Clarendon, Oxford, 1997.
3. Yupapin, P. P., W. Suwanchareon, and S. Suchat, "Nonlinearity penalties and benefits of light traveling in a fiber optic ring resonator," *Int. J. of Light and Electron. Opt.*, 2007.
4. Yupapin, P. P. and N. Pornsuwancharoen, *Guided Wave Optics and Photonics: Microring Resonator Design for Telephone Network Security*, Nova Science Publishers, New York, 2008.
5. Yupapin, P. P. and P. Saeung, *Photonics and Nanotechnology*, World Scientific, Singapore, 2008.
6. Su, Y., F. Liu, and Q. Li, "System performance of slow-light buffering and storage in silicon nano-waveguide," *Proc. SPIE*, Vol. 6783, 68732, 2007.
7. Gharakhili, F. G., M. Shahabadi, and M. Hakkak, "Bright and dark soliton generation in a left-handed nonlinear transmission line with series nonlinear capacitors," *Progress In Electromagnetics Research*, PIER 96, 237–249, 2009.
8. Ballav, M. and A. R. Chowdhury, "On a study of diffraction and dispersion managed soliton in a cylindrical media," *Progress In Electromagnetics Research*, PIER 63, 33–50, 2006.
9. Konar, S. and A. Biswas, "Soliton-soliton interaction with power law nonlinearity," *Progress In Electromagnetics Research*, PIER 54, 95–108, 2005.
10. Gangwar, R., S. P. Singh, and N. Singh, "Soliton based optical communication," *Progress In Electromagnetics Research*, PIER 74, 157–166, 2007.
11. Yupapin, P. P., N. Pornsuwanchroen, and S. Chaiyasoonthorn, "Attosecond pulse generation using nonlinear microring resonators," *Microw. and Opt. Technol. Lett.*, Vol. 50, 3108, 2008.
12. Kivshar, Y. S. and B. Luther-Davies, "Dark optical solitons: Physics and applications," *Phys. Rep.*, Vol. 298, 81, 1998.
13. Sangwara, N., K. Sarapat, K. Srinuanjan, and P. P. Yupapin, "A novel dark-bright optical solitons conversion system and power amplification," *Opt. Eng.*, Vol. 48, No. 4, 045004, 2009.
14. Zhao, W. and E. Bourkoff, "Propagation properties of dark solitons," *Opt. Lett.*, Vol. 14, 703, 1989.
15. Barashenkov, I. V., "Stability criterion for dark soliton," *Phys.*

Rev. Lett., Vol. 77, 1193, 1996.

16. Christodoulides, D. N., T. H. Coskun, M. Mitchell, Z. Chen, and M. Segev, "Theory of incoherent dark solitons," *Phys. Rev. Lett.*, Vol. 80, 5113, 1998.
17. Kim, A. D., W. L. Kath, and C. G. Goedde, "Stabilizing dark solitons by periodic phase-sensitive amplification," *Opt. Lett.*, Vol. 21, 465, 1996.
18. Malomed, B. A., A. Mostofi, and P. L. Chu, "Transformation of a dark soliton into a bright pulse," *J. Opt. Soc. Am. B*, Vol. 17, 507, 2000.
19. Fietz, C. and G. Shvets, "Nonlinear polarization conversion using microring resonators," *Opt. Lett.*, Vol. 32, 1683, 2007.
20. Kokubun, Y., Y. Hatakeyama, M. Ogata, S. Suzuki, and N. Zaizen, "Fabrication technologies for vertically coupled microring resonator with multilevel crossing busline and ultracompact-ring radius," *IEEE J. of Sel. Topics in Quantum Electron.*, Vol. 11, 4, 2005.
21. Mithata, S., N. Pornsuwancharoen, and P. P. Yupapin, "A simultaneous short wave and millimeter wave generation using a soliton pulse within a nano-waveguide," *IEEE Photon. Technol. Lett.*, Vol. 21, No. 13, 932, 2009.
22. Yupapin, P. P., P. Saeung, and C. Li, "Characteristics of complementary ring-resonator add/drop filters modeling by using graphical approach," *Opt. Commun.*, Vol. 272, 81, 2007.
23. Yupapin, P. P. and W. Suwancharoen, "Chaotic signal generation and cancellation using a microring resonator incorporating an optical add/drop multiplexer," *Opt. Commun.*, Vol. 280, 343, 2007.
24. Hanim, S. F., J. Ali, K. Thambiratnam, H. Ahmad, and P. P. Yupapin, "An experimental investigation of dark soliton generated by using S-band erbium doped fiber amplifier," *Optical Engineering*, 2009 Submitted.
25. Fujii, M., J. Leuthold, and W. Freude, "Dispersion relation and loss of subwavelength confined mode of metal-dielectri-gap optical waveguides," *IEEE Photon. Technol. Lett.*, Vol. 21, 362, 2009.
26. Yupapin, P. P. and N. Pornsuwanchroen, "Proposed nonlinear microring resonator arrangement for stopping and storing light," *IEEE Photon. Technol. Lett.*, Vol. 21, No. 6, 404, 2009.